Semester project report

Measurement and comparison of graphene-based resonant accelerometers

---

Author:
Driss Belkass

Instructor:
Villanueva Torrijo Luis Guillermo

Assistant:
Moreno Garcia Daniel

June 11, 2021

Abstract

An accelerometer is a device used to measure acceleration. Acceleration is the rate of change of an object's velocity, measured in square meters per second $[m/s^2]$ or **g** force. This type of device is used to detect vibrations or the orientation of certain systems. We can find accelerometers in many fields like engineering or industry.

Today accelerometers are very much expected in the fields of biology and biomechanics, that said for these fields the devices must become smaller and smaller to be able to respond to the problem encountered in this sector, for example to equip micro-ships that could be used in the human body and thus help in their navigation.

In this project we will try to test accelerometers that could address this important issue. These accelerometers are developed at KTH[1] Royal Institute of Technology, they are the smallest accelerometer today, they have been designed with a graphene membrane that supports a silicone proof mass. They belong to the category of Nano-Electro-Mechanical Systems (NEMS).
We studied different types of masses (different shapes and sizes) and under different conditions. Firstly to see if we could verify some form of repeatability in the devices and if we were close to the theoretical results. And secondly to see if one configuration was better than the others.

The results show that the circles masses were way more effective and that the sizes did not really affect the results. And we also showed that the annealing and the clamping had a important effect on the devices.

Contents

1 Introduction

Actual mechanical accelerometers are usually small Micro-Electro-Mechanical systems (MEMS), and are usually very simple devices consisting only of a cantilever with test quality. As today we are trying to get smaller and lighter, the new accelerometers developed by KTH, that we will test during this study, are important players for the future. This will open new doors to the world of the nano scale, we will have more information to understand or control the new inventions in this scale.

It is thanks to the exceptional characteristics of graphene that this new type of accelerometer have been developed. The devices consists of a thin layer of CVD graphene ribbons to which is attached a proof mass made of silicon. The graphene is studied as resonators since its resonant frequency is mostly controlled by in-plane tension thanks to its small thickness. Indeed, the graphene layers are normally about one atom thick so it is therefore usually thin. The principle of this device is that when applying an acceleration the proof mass creates a force that affects the graphene structure. This new force, due to the acceleration, results in a stress change of the graphene layer. Moreover, we can notice this change in a shift in the resonant frequency of the device.
With the help of the resonant frequencies and the shift that appears, we can try to understand the mechanisms that take place in the accelerometer by calculating different parameters for each device like the responsivity, the stress membrane and more.

Our objectives during this study is: firstly, to try to explain and understand the theory behind these accelerometers. And secondly, we will analyse the data from the devices provided to us by KTH, so that we can compare them with each other and see if we can find any overall trends and links with the theory. And also try to find explanations for the results that emerge.

2 Accelerometers

2.1 Micro-ship

The accelerometers that we are going to use during the study are contained in a small micro-ship developed at KTH Royal Institute of Technology. The micro-ship we use was produced with two stacked sheets of single layer graphene from Graphenea (name of the company which produce the graphene) by making a PolyCarbonate (PC) based transfer. The name of the micro-ship is the following:

So, we can see from the name of the micro-ship **T3M202530CSR** the various characteristic of the devices, they have a trench of thickness 3 µm, there is three different sizes of proof mass (20 µm, 25 µm and 30 µm) and also three different shapes (circle, square and rectangle).

In the figure 1, we can see the plan of the micro-ship containing 225 devices (15 rows and 15 columns), where every line is composed by a different type of accelerometer, with either a different size or a different shape.
During the study, we named each device as : row x column.

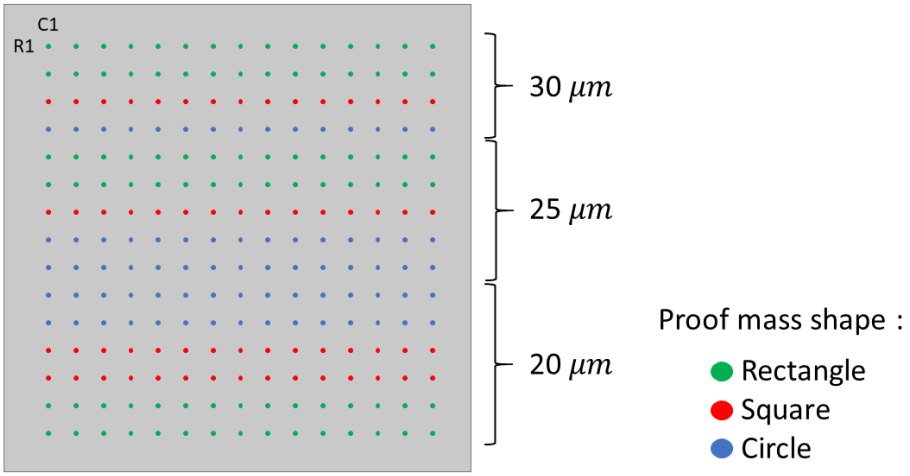

Fig. 1: Plan of the micro-ship: T3M202530CSR

We have therefore concentrated our research on this micro-ship, as we can more easily compare a large number of different types of NEMS accelerometer. Also, since the same

type of device is repeated at least 15 times, we can get an idea of the repeatability and have fairer average values.

2.2 Devices structure

As we can see in the figure 2**a**, the accelerometer consists of a double layer of graphene stretched and tied at all ends. To this stretched layer of graphene is therefore attached from below a proof mass made of SiO_2 and Si. The gap between the attachment ends of the graphene layer and the proof mass is the trench, as we see it in the figure 2**b** that represent therefore the graphene in suspension.

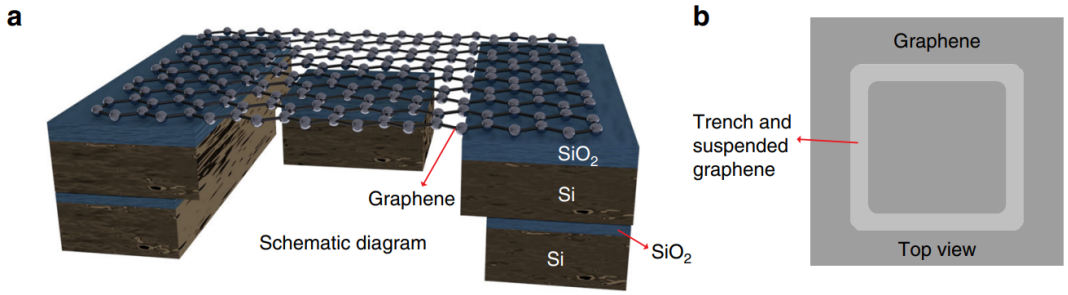

Fig. 2: 3D diagrams of the structures and SEM images. **a** 3D schematic of the graphene membrane with a suspended proof mass. **b** 3D schematic top view[2]

3 Theory

In order to understand the theory we must first explain our model which we will analyse and how it is affected. Then we will focus on the important points related to this model that will be relevant for the study later.

The accelerometer as explained in the previous part is made of a graphene layer to which we have suspended a proof mass, when this one is affected by an acceleration it will create a force which will pull on the graphene. The graphene membrane submitted to this force will be moved i.e. displacement will appear and moreover we will see more membrane stress appear in it. Therefore, this change in tension create also a change in the resonant frequency.

Now that we understand the system, we need to create a model that can be used for this study. As shows the scheme in the figure 3 and as we explain earlier the force from the displacement of the proof mass suspended at the graphene applied on the centre of mass. Plus, we consider the two external parts of SiO_2/Si as fixed supports to the graphene membrane, therefore tension appears in the membrane since it is enclosed to the outside.

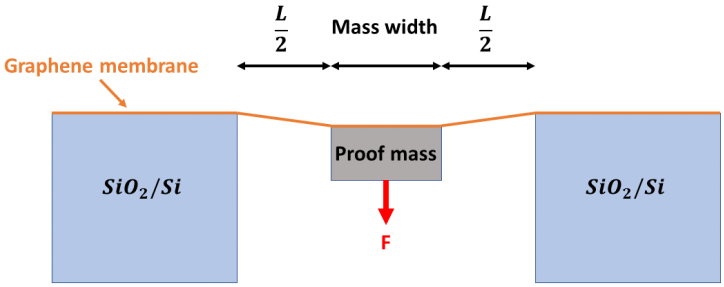

Fig. 3: Model scheme for the theoretical study

By seeing the diagram (figure 3), we can quickly see that we can simplify the model by removing the mass because it is symmetrical and the force is applied to its center. Thus the size of the suspended graphene layer is twice the size of the trench, i.e. L ($\frac{L}{2} + \frac{L}{2}$).

3.1 Resonant frequency

To find the theoretical results of this model we were inspired by studies where was used more general solutions of a load-deflection system and where were also determine the missing coefficients by doing FEM (finite element simulations).
In order to find the resonant frequency we need to find the variables that are in the natural frequency equation of the system that we know: $k = (2\pi f_R)^2 m$
Where m represents the mass and k represents the stiffness that is obtain by deriving the force by the displacement : $k = \frac{dF}{dz}$

So to find the force we first find the pressure P present in the membrane, then we know that the Force $F = P \cdot Area$, where the area depends on the shape of the device's proof mass and that represents the suspended graphene membrane :

Proof mass shape	Area
Square	$(W_{mass} + L)^2 - W_{mass}^2$
Rectangle	$LW_{mass} + LU_{mass} + L^2$
Circle	$\pi(LW_{mass} + L^2)$

Where W_{mass} and U_{mass} are respectively the width and the longer of the proof mass.

Thus thanks to the general formulas of load-deflection system we can obtain the pressure equation P [3]:

$$P = \frac{C_{Tension}H}{L^2}\left(\sigma_0 + \frac{C_{lin}}{C_{Tension}}\left[\frac{EH^2}{(1-\nu^2)L^2}\right] + \frac{C_{nlin}}{C_{Tension}}\left[\frac{E}{(1-\nu^2)L^2}\right]Z^2\right)\cdot Z \quad (1)$$

Where H the thickness of the membrane, σ_0 the membrane stress, ν the Poisson's ratio and the geometry coefficients C_{lin}, C_{nlin} and $C_{Tension}$. And Z is the membrane displacement which can be expressed as follows: $Z = \frac{m \cdot a}{Area \cdot \frac{C_{Tension}H}{L^2}\sigma_0}$

And finally, by going through the developments we have just explained we can find the frequency of resonnance f_R:

$$f_R = \frac{1}{2\pi}\sqrt{\frac{Area \cdot C_{Tension}H}{mL^2}\left[\sigma_0 + \frac{C_{nlin}}{C_{Tension}}\frac{EH^2}{(1-\nu^2)L^2} + \frac{3 \cdot C_{nlin}}{C_{Tension}}\frac{E}{(1-\nu^2)L^2}\left(\frac{ma}{Area \cdot \sigma_0 \frac{C_{Tension}H}{L^2}}\right)^2\right]} \quad (2)$$

3.2 Responsivity

The Responsivity is the parameter that will help us compare the devices, it gives us an idea on the quality as an accelerometer. It helps us quantify the shift in the resonant frequency (f_R) coming from the acceleration that affects the device. So the more the device is affected by the acceleration the higher the responsivity will be.

$$R = \frac{1}{f_R(g)} \cdot \left.\frac{\delta f_R}{\delta a}\right|_g \quad (3)$$

In the equation, we evaluate the responsivity in relation to the variable g which corresponds to the gravity of the Earth. We take it into account because it always brings a bias to our measurement.

3.3 Membrane stress

To find the membrane stress we use the equation 2. By developing the equation to bring out σ_0, we find a third order equation (see the development appendix A):

$$-\sigma_0^3 + \left(\frac{4\pi^2 f_R^2 \cdot mL^2}{Area \cdot C_{Tension} H} - \frac{C_{nlin}}{C_{Tension}} \frac{EH^2}{(1-\nu^2)L^2}\right)\sigma_0^2 - \frac{3 \cdot C_{nlin}}{C_{Tension}} \frac{E}{(1-\nu^2)L^2} \left(\frac{ma}{Area \cdot \frac{C_{Tension} H}{L^2}}\right)^2 = 0 \tag{4}$$

So, our coefficients for the third order equation are:

$$a \cdot \sigma_0^3 + b \cdot \sigma_0^2 + c \cdot \sigma_0 = Constant$$

Coefficient	**a**	-1
	b	$\frac{4\pi^2 f_R^2 \cdot mL^2}{Area \cdot C_{Tension} H} - \frac{C_{nlin}}{C_{Tension}} \frac{EH^2}{(1-\nu^2)L^2}$
	c	0
Constant		$\frac{3 \cdot C_{nlin}}{C_{Tension}} \frac{E}{(1-\nu^2)L^2} \left(\frac{ma}{Area \cdot \frac{C_{Tension} H}{L^2}}\right)^2$

We also calculated the membrane stress for some devices using a matlab code (See appendix B.1).

4 Measurement

In this part we will explain all the tools we used in our study, presenting the experimental materials and the method by which all the measurements were analysed.

For the study we needed to measure the Responsivity, as we saw in the equation 3 it gives us an important idea on the shift magnitude in relation to the acceleration that affects the device. To do so, here in the figure 4 the setup that we made to be able to measure the shift in resonance frequency of the device.

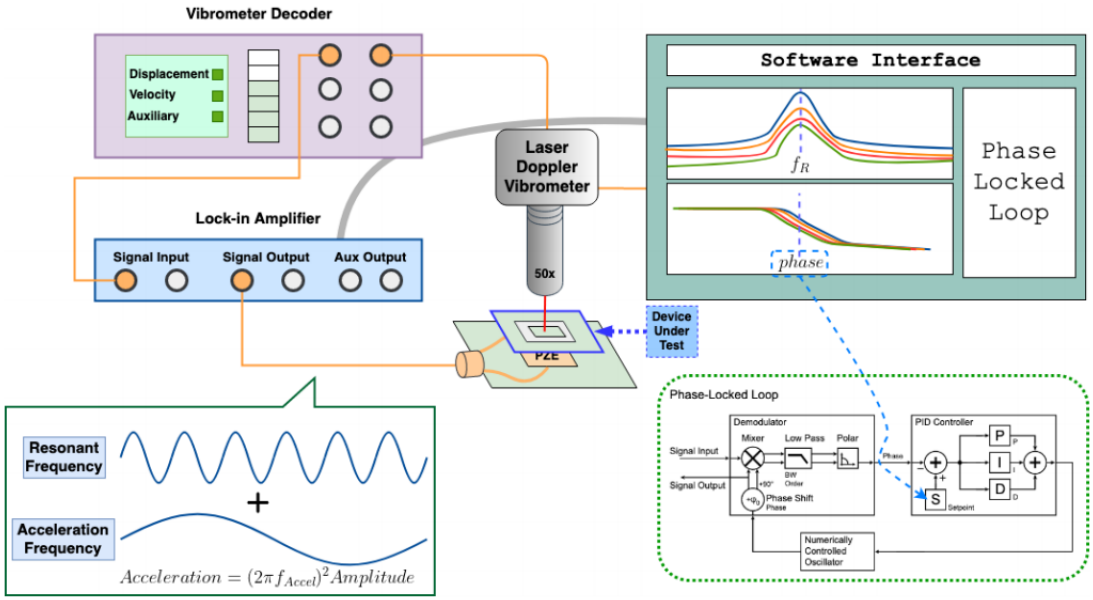

Fig. 4: Complete set-up to measure displacements and velocities from the Device Under Test (DUT). It is based on a Laser Doppler Vibrometer, a Vibrometer Decoder and a Lock-in amplifier. The goal is to excite the resonance of the DUT and to add an acceleration signal while measuring the resonant frequency changes.[4]

The micro-ship with the devices lies on a piezo-shaker. It converts a signal into vibrations, thanks to this the piezo-shaker excites the accelerometer to its resonant frequency. Plus, a low frequency signal is sent to the piezo-shaker which correspond to a wanted acceleration. The Laser Doppler Vibrometer is above the micro-ship while its signal is sent to the Vibrometer Decoder which performs transformations so that the Lock-in amplifier can display the results on the computer.

4.1 Tools

- **Laser Doppler Vibrometer (LDV)**: OFV-551 Fiber-Optic Sensor Head
- **Lock-in Amplifier**: Zurich instruments, UHFLI 600 MHz Lock-in Amplifier
- **Vibrometer Decoder**: Polytec OFV-5000 Vibrometer Controller
- **Piezo-shaker**
- **Camera and optical microscope lens**: lens from Mitutoyo (20X)

4.2 Laser Doppler Vibrometer (LDV)

The LDV is the methods that gives us the best displacement and velocity measurements, it allows to detect a change of amplitude at the scale of the femtometer.
It uses the Doppler effect to measure vibration, if the laser is reflected by a moving object its frequency is changed slightly, and the frequency shift that we measure can be expressed as : $f_D = 2 \cdot \frac{v}{\lambda}$

The interferometer splits the laser into two parts, one that points directly to the photo detector and the other is incident to the test object, where the Doppler effect happens, then comes back to the photo detector.
Then finally, the signal processing and analysis of the superposition of both parts reveals the displacement and the vibration velocity of the test object.

4.3 Thermomechanical noise

The first step with the computer, after pointing with the laser thanks to a camera to a device, is to find the resonant frequency. To do so, we read the output of the LDV on the software interface, it shows us the thermomechanical noise and a peak at as in the figure 5 that represents the resonant frequency of the device.

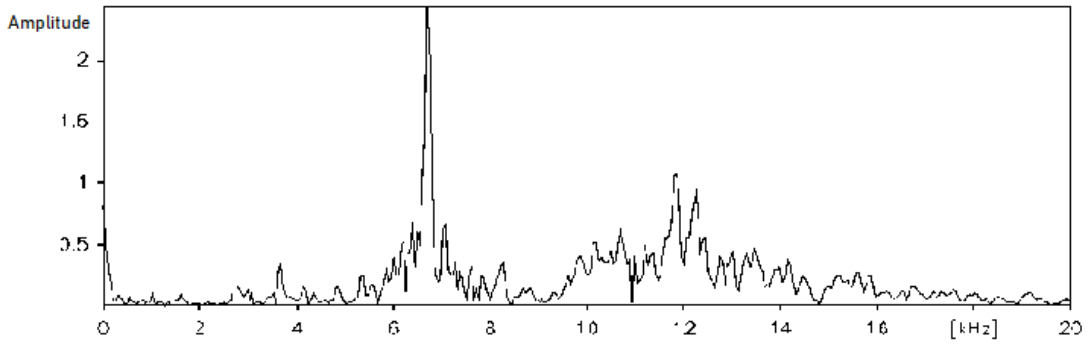

Fig. 5: Resonances of the devices can be seen, Fast Fourier Transform (FFT) is used.[5]

Then we do a single plot pass to analyse more precisely the peak and to find at which voltage the signal has maximal information.

4.4 Sweep in Frequency

In this step we determined the resonant frequency, and now we apply an excitation with the piezo-shaker at different voltages. We could see that the more the voltage is important the more the amplitude will be high. But we must be careful not to take a voltage too high for the study to not lose information. Indeed, when the voltage exceeds a threshold the peak becomes more and more tilted and we lose information in the signal, the figure 6 explains the phenomenon well.

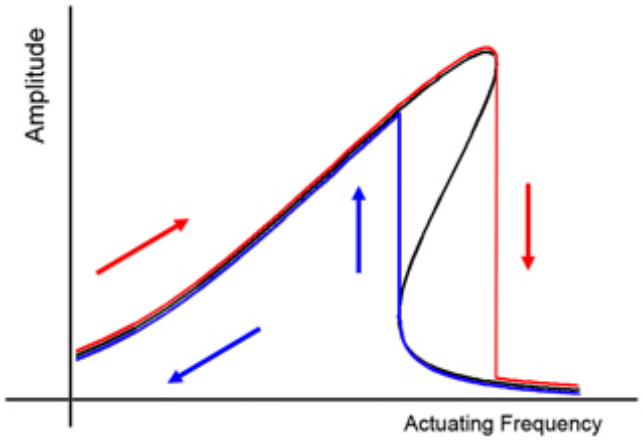

Fig. 6: Sweep in frequency brief sketch explaining how we can lose information during the sweep in frequency.[6]

Then we automated the process with a matlab code that was written by Daniel Moreno (See appendix B.2). It is also important to remember that before doing this we must proceed to an autocalibration of the micro-ship because this one will also have an acceleration (also made with a matlab code B.3).

4.5 Measurement of the Responsivity

To measure the responsivity we find out thanks to the sweep in frequency the value of the shift in resonant frequency (Δf_R) for each acceleration (a). And as we explain earlier in the part 3.2, the responsivity corresponds to the change of the shift in resonant frequency in relation to the acceleration divided by the resonant frequency. And that can be represented by the slop of the function of Δf_R against a divided by f_R.

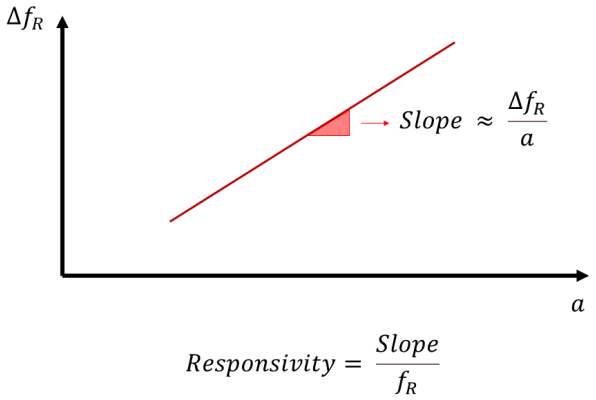

Fig. 7: Finding the Responsivity thanks to slope of Δf_R vs a.

To find the slope we used to different methods. For the first one, we used the Excel software which allowed us to plot the points of our measurement, and then find a linear

trend which we brought out the equation from and thus the value of its slope (see figure 8).

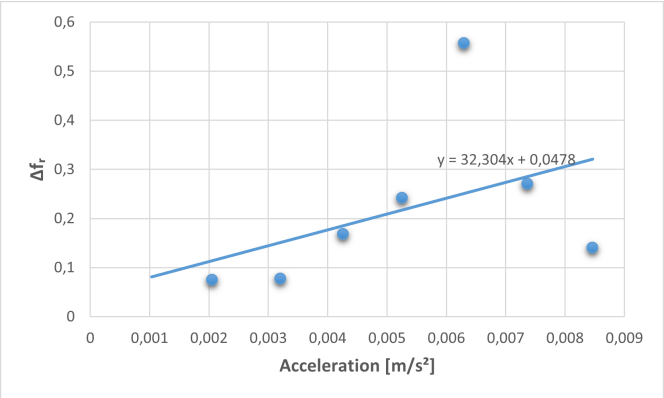

Fig. 8: Example to bring out the linear trend to find the responsivity of the device.

For the second method, we created a matlab code that also finds a linear trend in the result and gives as output the slope of the curve (see appendix B.4).

4.6 Allan deviation and Noise

Thanks to the Allan deviation, we can have another idea of an important parameter of the accelerometer : the minimum acceleration value that the tool can detect. Indeed, the Allan deviation is directly related to the minimum acceleration:

$$Allan\ deviation = a_{min} \cdot Responsivity \tag{5}$$

Moreover, we want to finds the lowest integration time that produces the lowest noise in the reading of the device data. The Allan deviation (σ_y) is calculated as that for N measurements of T_i and sampling period τ_0 [7],

$$\sigma_y(\tau_0) = \sqrt{\frac{\sum_{i=1}^{N-1}(T_{i+1} - T_i)^2}{2(N-1)}} \tag{6}$$

By averaging n adjacent values of T_i so that $\tau = n\tau_0$ means that the sampling period is varied and we have,

$$\sigma_y(\tau) = \sqrt{\frac{\sum_{i=1}^{N-2n+1}(T_{i+2n} - 2T_{i+n} + T_i)^2}{2\tau^2(N-2n+1)}} \tag{7}$$

So, there is a matlab code (see appendix B.5) that helps us find the Allan deviation for our data. We used it for one set of that since it will give us similar results each time. We can therefore see in the figure 9, that we have a minimal noise effect for an integration time lower than 0,1 second. This shows us how fast can be the sensor.

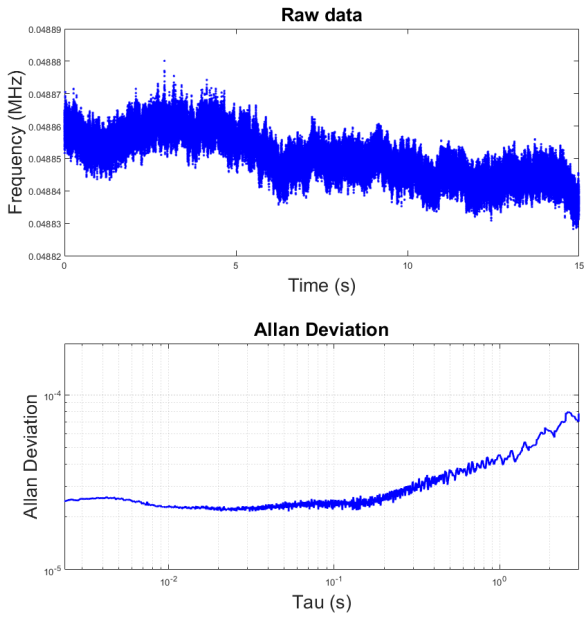

Fig. 9: Allan deviation plot, helps us find the best integration time for the study.

4.7 Acceleration

4.7.1 Shift in frequency

To find the shift in acceleration, as explained above, a small acceleration is sent by signal to the piezo shaker in addition to the resonance signal.
The signal shown in the figure 10 gives us the amplitude of the FFT. At 160 Hz which corresponds to the frequency of the actuation, we can notice a spike that shows the effect of the acceleration on the resonant frequency of the device, that's what we are going to measure.

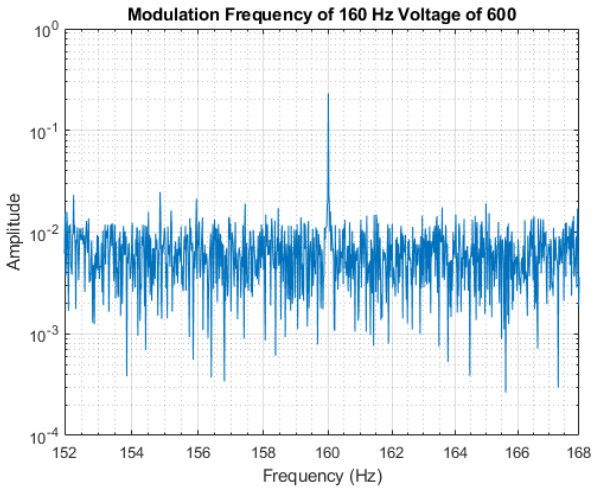

Fig. 10: FFT (Fast Fourier Transform) of the data centered at 160 Hz which is the frequency at which we send the small acceleration.

4.7.2 Minimum acceleration

To find the minimum acceleration for each device which will give us an additional quality parameter for the comparison, there is to step to follow.

The first step is to find the level of the noise where the peak of acceleration cannot be seen. To do so, we take the second biggest peak after the one at 160 Hz corresponding to the acceleration effect as you can see in the figure 11a, where the second peak is shown by the red cross.
For the second step, knowing the linear slope of Δf_R against acceleration (as explained in the part 4.5) and the noise level found in the first step, we can interpolate the function as shown in the figure 11b to find out the minimum acceleration.

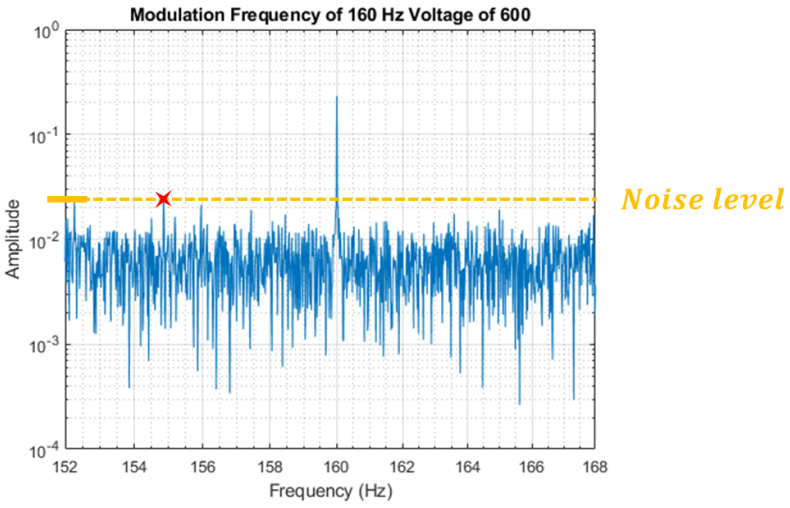

(a) First step

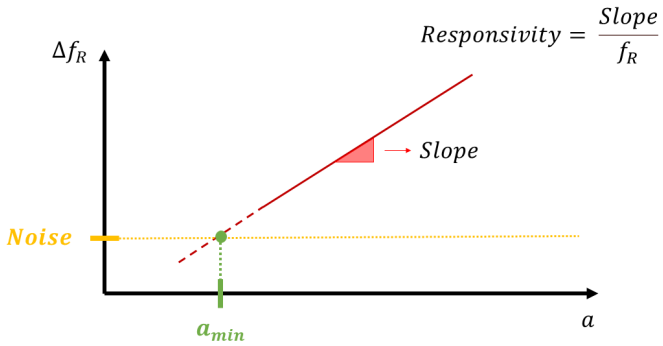

(b) Second step

Fig. 11: Method for finding the minimum acceleration thanks to the Noise that we know through the FFT.

5 Results

In this part we will show all the results we have acquired during our study. There were three different important steps in our project, where the micro-ship was put under different conditions. (See also appendix C)
First of all, we were very interested in the responsivity which is a parameter that tells us a lot about the quality of our accelerometers.

5.1 Not clamped

At the beginning we took the micro ship as such, and thus took first measurements which was going to be used to us as standard for the continuation of the research. We took many measurements, for the three different shapes and sizes of 20 and 30 µm. The measurements were taken each time on several devices of the same type in order to have more accurate average results to find real trends.

In the figure 12, we can see the first results we had during our research and they will be interesting to compare later. We can also see on this same graph that these are averages, so there is a standard deviation that gives us an idea of the overall values. Moreover, we can see that for the rectangles mass 20 the standard deviation becomes even negative, this is not a error but in the measurements we had for a case a negative tendency for the measured points as in the figure 8.

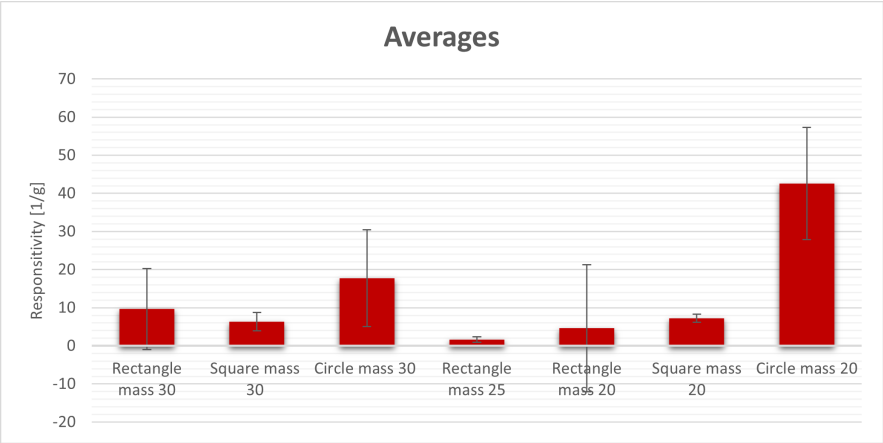

Fig. 12: Average measurements of responsivity for different types of devices with the micro-ship without clamping.

5.2 Clamping with glue

In this part knowing that the micro-ship is directly put on the piezo shaker all the system is subjected to the vibration, to mitigate this we thought of bringing a change to the micro-ship. This change is simply the idea of gluing the micro-ship with glue to two small thin pieces of metal. So this should alleviate the problem.

We thus repeated the measurements on exactly the same devices as we saw in the part 5.1, in order to be able to compare the results well (see figure 13).

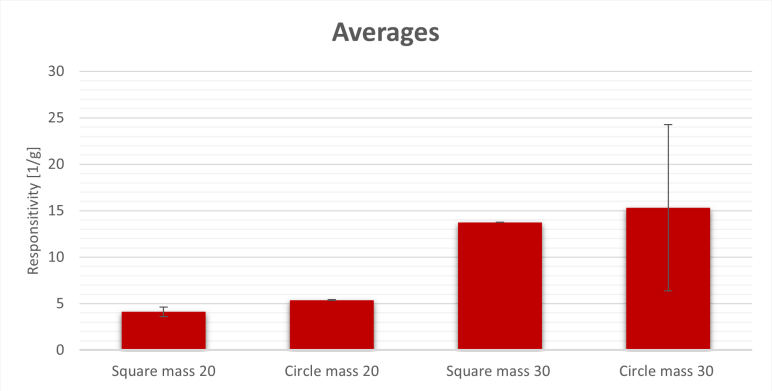

Fig. 13: Average measurements of responsivity for different types of devices with the micro-ship clamped with glue.

5.3 Annealing

For the last step, we decided to put the micro-ships under vacuum in order to have the minimum of impurities because at this scale the smallest impurity can be very disturbing. Another way to remove these impurities and to clean the graphene double layer, which is our main objective in this step, is to perform annealing.

The different stages of the annealing:

To bring the devices to an important temperature without damaging them and having the repercussions we want, we must follow different levels of warming up to reach our objectives.

Here are the different steps:

- Ambient temperature to 200°C, in 15 minutes
- 200°C to 350°C, in 20 minutes
- 350°C, during one hour

We then tried to find the resonant frequencies of the devices we had already measured in order to find the effect of the annealing on their graphene membrane. We can see in the figure 14 the resonance frequencies of 23 devices that we measured before and after the annealing steps that we explained above. In addition to that, for more clarity we have also put forward the trends to have a better visualization of the results.

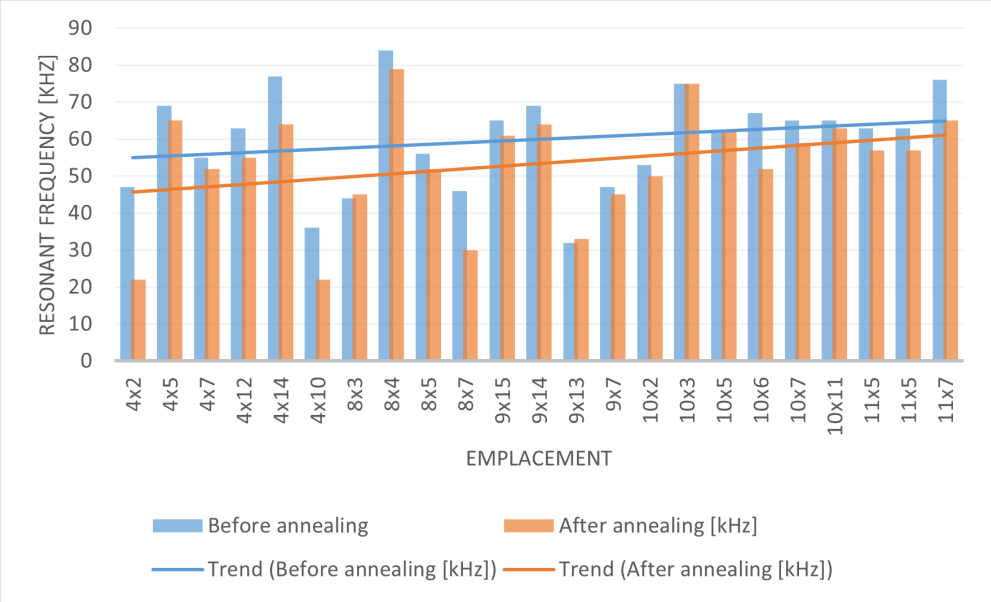

Fig. 14: Resonant frequency for different device, before annealing and after an annealing.

5.4 Minimum acceleration

For this part we decided to visualize the minimum acceleration of some device of different type in order to have an idea of the magnitude of these. In order to visualize the results we have decided to gather them in the following table:

Device name	Characteritics	f_R [kHz]	R [1/g]	a_{min} [m/s2]
1x8	Not clamped, rectangle mass 30	74	27.6	1.3462e-05
4x2	Not clamped, circle mass 30	53	23.28	0.00454
9x5	Not clamped, circle mass 25	56	37.67	0.006654
10x10	Not clamped, circle mass 20	104	22.46	2.4402e-04
4x2	Clamped, circle mass 30	47	9	0.00024
11x5	Clamped, circle mass 20	63	13.7	0.004543
13x5	Clamped, square mass 20	68	3.74	0.0018
4x5	Annealed, circle mass 30	71	4.46	9.9059e-04
9x7	Annealed, circle mass 25	47	52.8	4.0000e-04
10x5	Annealed, circle mass 20	62	13.8	0.00038

6 Discussion

6.1 Shape

In our study, the first result that immediately appeared to us was the higher responsivity of accelerometers with a cylinder-shaped proof mass.
As we can see in the figure 15, the responsivity is about 3 times higher than the square and rectangle.

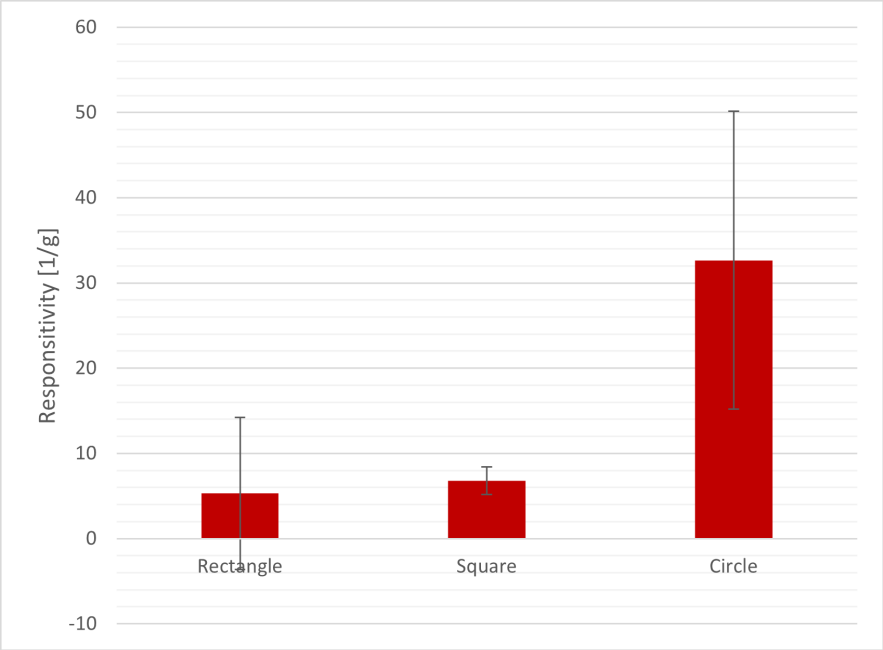

Fig. 15: Average measurements of device's responsivity for different shapes with the micro-ship not clamped.

We can explain this perhaps by the fact that for the proof mass in the shape of rectangle and square, that there are perhaps more internal bending in the proof mass due to their shape that allows it more than for those in circle.

6.2 Mass size

The second thing we noticed was that the size of the proof mass (20 µm, 25 µm and 30 µm) didn't really matter for the responsivity. As we can see in the figure 16, we see that for all types of proof mass, by focusing only on their size there is no real difference or trend that shows up. The differences in size are probably not significant enough to make a big difference to the responsivity.

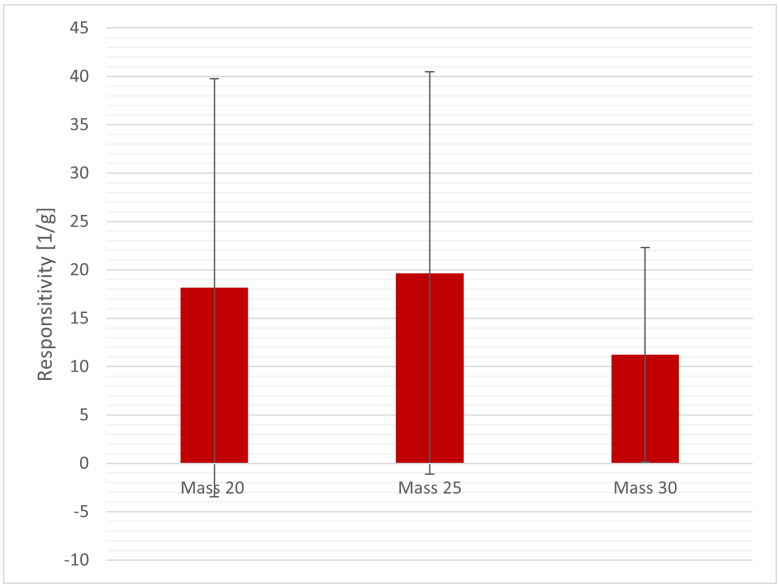

Fig. 16: Average measurements of device's responsivity for different mass sizes with the micro-ship clamped with glue.

To confirm this result, as we have seen in the part 6.1 that the circles had a more interesting responsivity, we decided to focus on those. And we can see that the same result comes out (see figure 17), so we can say that the size differences have no real impact here.

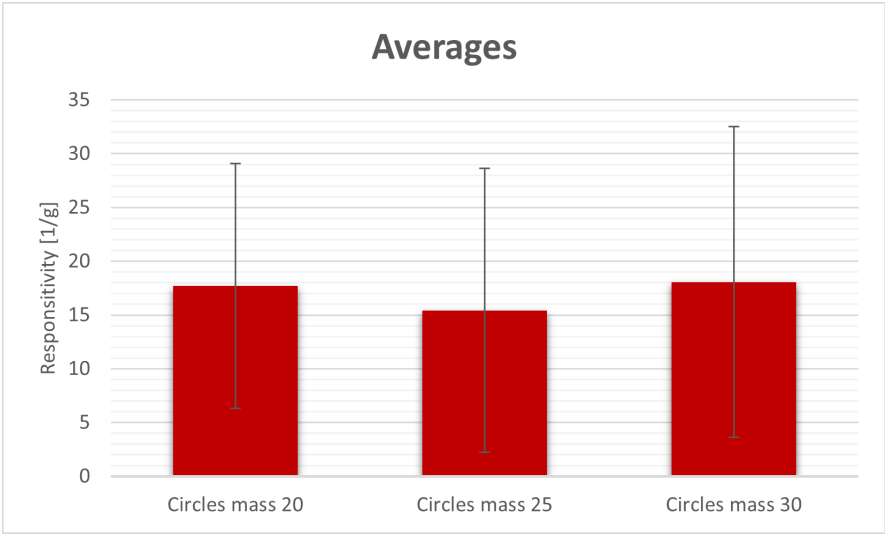

Fig. 17: Average measurements of device's responsivity with different circles mass sizes with the micro-ship clamped with glue.

6.3 Clamping

By gluing the micro-ship to two small metal plates we wanted to check if the results we found would follow in our studies. In this case the micro-ship is bonded to the 2 metal plates. Since the micro-ship is more clamped, normally one would notice that the displacement of the devices should be reduced because of this clamping. Therefore, if

the device makes less displacement, it should respond less to the acceleration sent by the piezo-shaker and so we should have smaller responsivity. This is what we have found for the majority of our measurements as shown in the figure 18. We can thus think that our measurements give us very interesting results.

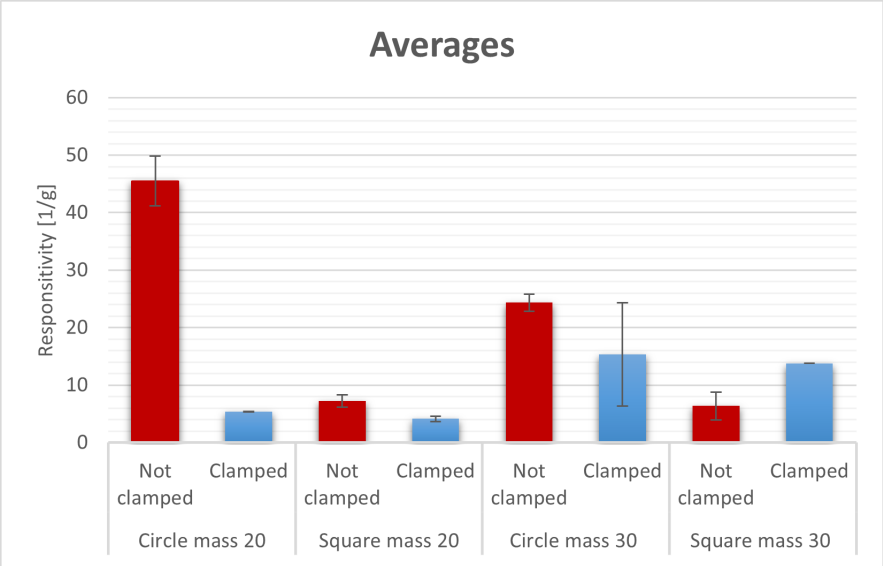

Fig. 18: Comparison of average measurements of device's responsivity for clamped and not clamped micro-ship.

6.4 Membrane stress

Thanks to the figure 19, we saw that for all the sizes of devices with the circle proof mass, we have the same trend. The higher the membrane stress, the higher the resonant frequency. Having less stress, the membrane is less subject to constraint and will be able to move more and therefore the resonance frequencies should be greater, this is what explains the trends in the graph 19.

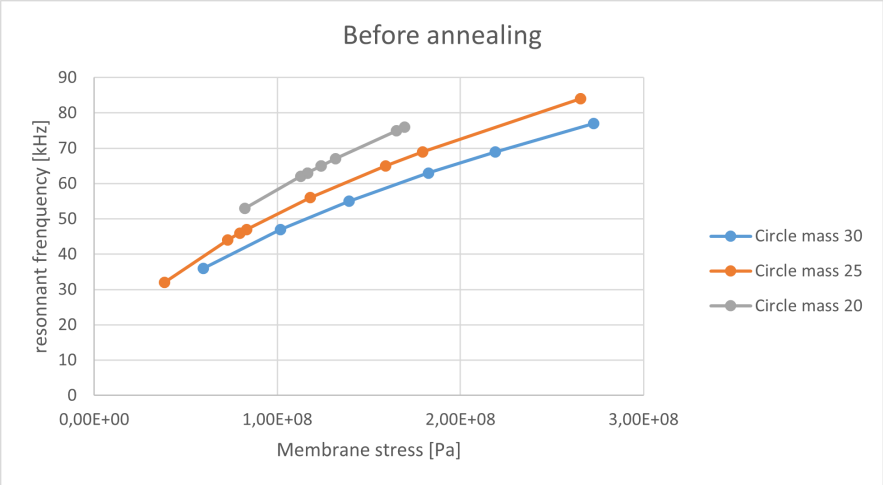

Fig. 19: Resonant frequency against membrane stress for circle proof masses of 20 µm, 25 µm and 30 µm.

6.4.1 Releasing stress

Doing annealing allowed us, first of all to clean the graphene membrane from residues as we explained in the section 5.3, but it would also allow us to decrease the stress in the membrane.

Indeed, we know that "Thermal annealing affects the resonators in two ways: (i) it relaxes the graphene sheets due to the thermal cycling, and (ii) it removes the residues. The latter point makes all membranes close to the pristine case, therefore the dispersion is much smaller and the estimation is more accurate, since the mass-loading effect of the residues disappears."[8]

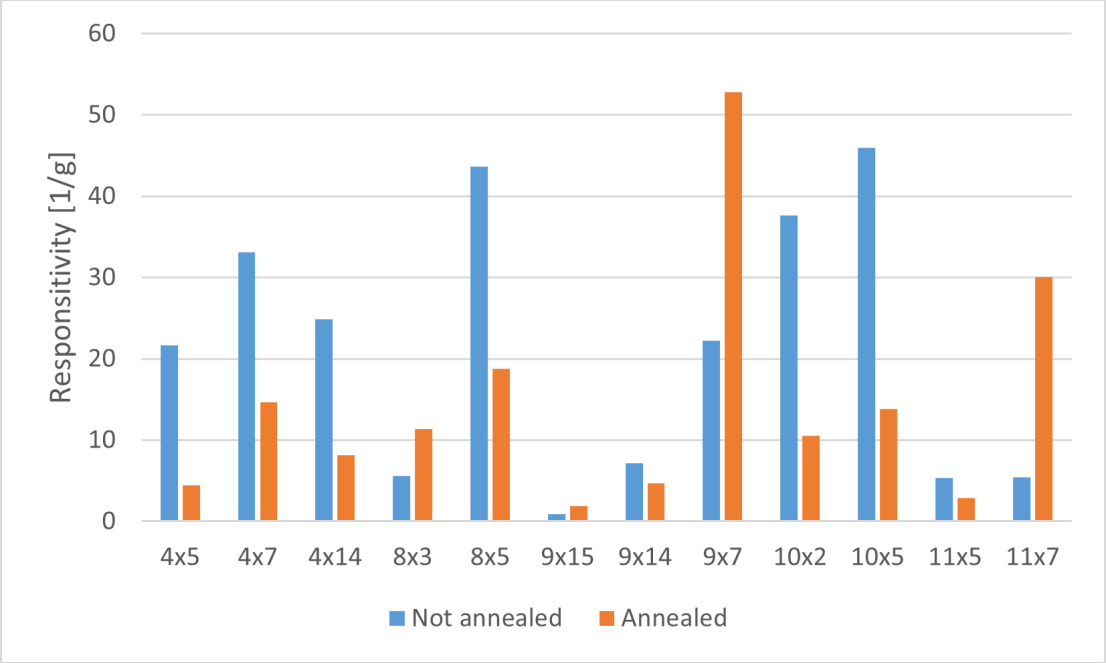

Fig. 20: Comparison device's responsivity for annealed and not annealed micro-ship.

However, as shown in the figure 20, we have not seen any real impact on the responsiveness of the devices.
We also can see that there is no real trends that shows up when we see the the responsivity against the membrane stress (see figure 21).

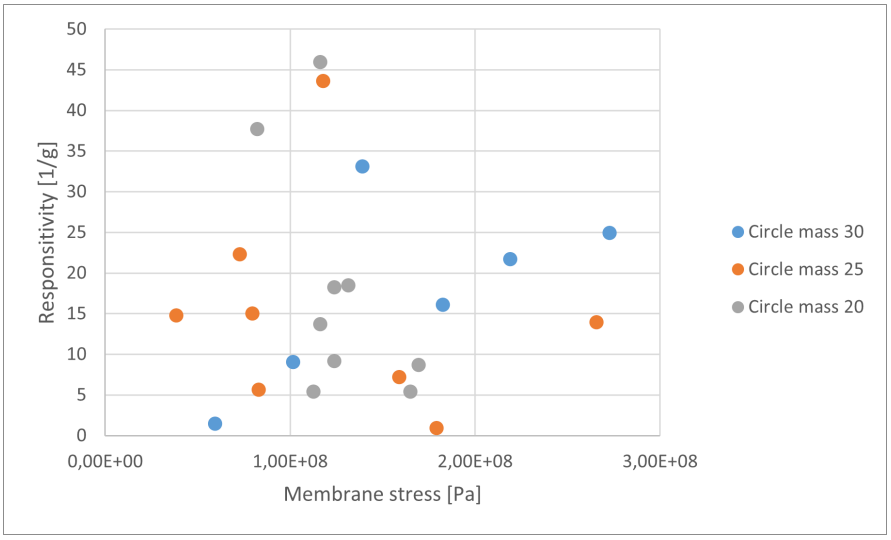

Fig. 21: Responsivity against membrane stress for circle proof masses of 20 µm, 25 µm and 30 µm.

7 Conclusion

During our study, we employed all our resources using a complete setup that allowed us to successfully create an important data set to analyze.

Indeed with this setup, we were able to analyze data from accelerometers of different sizes and shapes. But even more, we measured the accelerometers under different conditions which showed that our results made sense.
Our results have shown that the shape of the proof mass and the various conditions in which the accelerometers are placed have a significant impact on their characteristics. These changes can impact the responsivity or the stress in the graphene membrane of our devices.

For further research in this area, we think that developing the setup to be more automated in order to verify and compare measurements on a larger number of devices could be interesting. This would help us to better check the repeatability aspect, but also to have more results and thus more apparent trends.

We have proven in part that these accelerometers are indeed very efficient at detecting small vibrations, and this is an important advance for the future that will allow us to detect these phenomena in smaller and smaller systems.

8 References

[1] Peter Ardell/David Callahan. World's smallest accelerometer points to new era in wearables, gaming, Sep 02, 2019.

[2] Fan Xuge, Smith Anderson D., Forsberg Fredrik, Wagner Stefan, Schröder Stephan, Shirin Afyouni Akbari Sayedeh, Fischer Andreas C., Villanueva Luis Guillermo, Östling Mikael, Lemme Max C., and Niklaus Frank. Manufacture and characterization of graphene membranes with suspended silicon proof masses for mems and nems applications. *Microsystems & Nanoengineering*, 6(17), 2020.

[3] Daniel Moreno. Modelling, simulations and characterization of nanoelectromechanical accelerometers based on graphene. 2020.

[4] Moreno Daniel, Fan Xuge, Niklaus Frank, and Villanueva Luis Guillermo. Proof of concept of a graphene-based resonant accelerometer. *34th International Conference on Micro Electro Mechanical Systems (MEMS)*, 2021.

[5] Grosse Christian U. and Reinhardt Hans W. The resonance method - application of a new nondestructive technique which enables thicknfss measurements at remote concrete parts. 1(10), 1992.

[6] Seung Sae Hong. Nanoelectromechanical system (nems): Observing mechanical nonlinearity, October 31, 2007.

[7] Land D V, Levick A P, and Hand J W. The use of the allan deviation for the measurement of the noise and drift performance of microwave radiometers. *Measurement Science and Technology*, 18(7), 2007.

[8] Akbari Shirin Afyouni, Ghafarinia Vahid, Larsen Tom, Parmar Marsha M., and Villanueva Luis Guillermo. Large suspended monolayer and bilayer graphene membranes with diameter up to 750 µm. *Scientific Reports*, 10(6426), 2020.

Appendices

A Membrane stress equation

$$f_R = \frac{1}{2\pi}\sqrt{\frac{Area \cdot C_{Tension} H}{mL^2}\left[\sigma_0 + \frac{C_{nlin}}{C_{Tension}}\frac{EH^2}{(1-\nu^2)L^2} + \frac{3 \cdot C_{nlin}}{C_{Tension}}\frac{E}{(1-\nu^2)L^2}\left(\frac{ma}{Area \cdot \sigma_0 \frac{C_{Tension} H}{L^2}}\right)^2\right]}$$

$$\frac{4\pi^2 f_R^2 \cdot mL^2}{Area \cdot C_{Tension} H} = \sigma_0 + \frac{C_{nlin}}{C_{Tension}}\frac{EH^2}{(1-\nu^2)L^2} + \frac{3 \cdot C_{nlin}}{C_{Tension}}\frac{E}{(1-\nu^2)L^2}\left(\frac{ma}{Area \cdot \sigma_0 \frac{C_{Tension} H}{L^2}}\right)^2$$

$$\frac{4\pi^2 f_R^2 \cdot mL^2}{Area \cdot C_{Tension} H} - \frac{C_{nlin}}{C_{Tension}}\frac{EH^2}{(1-\nu^2)L^2} - \sigma_0 - \frac{3 \cdot C_{nlin}}{C_{Tension}}\frac{E}{(1-\nu^2)L^2}\left(\frac{ma}{Area \cdot \frac{C_{Tension} H}{L^2}}\right)^2 \frac{1}{\sigma_0^2} = 0$$

$$-\sigma_0^3 + \left(\frac{4\pi^2 f_R^2 \cdot mL^2}{Area \cdot C_{Tension} H} - \frac{C_{nlin}}{C_{Tension}}\frac{EH^2}{(1-\nu^2)L^2}\right)\sigma_0^2 - \frac{3 \cdot C_{nlin}}{C_{Tension}}\frac{E}{(1-\nu^2)L^2}\left(\frac{ma}{Area \cdot \frac{C_{Tension} H}{L^2}}\right)^2 = 0$$

B Matlab code

B.1 Membrane stress

```
clear all
close all
warning off
%Inputs

Height=1.64E-05;              %[m]
t=0.000003;                   %trench [m]
L=0.000006;                   %[m]
C_Ten=4;
C_lin=15.90;
C_nlin=8;
H=6.7E-10;                   %tickness [m]
v=0.25;                      %poisson coef
E=2.2E11;                    %youngs modulus [Pa]
a=9.81;                      %acceleration [m/s^2]
p=2328;                      %Silicon density [kg/m^3]
f_R=22;                      %Resonnant frequency
f_R=f_R*1000;
W=36E-6;                     %Size measured
%U=;

%W=W*0.1714*10^(-6);         %Transformation scaling
%U=U*0.1714*10^(-6);

%membrane
%AreaMem=(W+L)^2-W^2;         %Square
AreaMem=pi*(W*L/2-L^2/4);  %Circle
%AreaMem=W*L+L*U-L^2;        %Rectangle

%Mass

%Vmass=(W-L)^2;               %area mass square
Vmass=pi*((W-L)/2)^2;        %Area mass circle
%Vmass=(W-L)(U-L);            %Area mass rectangle

m=p*Vmass*Height;            %mass

a=-1;
b=(4*pi^2*f_R^2*m*L^2)/(AreaMem*C_Ten*H)-((C_nlin)/(C_Ten))*((E*H^2)/((1-v^2)*L^2));
c=0;
d=-((3*C_nlin)/(C_Ten))*E/((1-v^2)*L^2)*((m*a)/(AreaMem*((C_Ten*H)/(L^2))))^2;

fplot(@(x) (-x^3+b*x^2+c*x+d),[-1000000000,1000000000]);
C=[a b c d];

x=roots(C);
abs(x(1))
```

B.2 Frequency sweep

```
clear all; close all;
device_id = 'dev2063';

VdriveResonance = 0.6;
FreqAcceleration = 160;

SamplingRate = 13e3;
%LowPassFilter = 10e3;

sweepPoints = 100;
StartFreq = 77e3;
EndFreq = 84e3;

SecondsPlotter = 60;

voltages = linspace(0.1,0.8, 8);


path = 'D:\Driss\New_generation\T3M20_25_30\5_2\'; Freq_shifts = [];
Freq_reson = [];
NoiseBIN = [];

index = 0;

for VdriveAccel = voltages index =
index+1;
LowPassFilter = 5*FreqAcceleration;

data = Sweeper(device_id, StartFreq, EndFreq, FreqAcceleration, 'amplitude', VdriveResonance, ↙
'sweep_samplecount', sweepPoints);

Sweep_freq = data.dev2063.demods.sample{1, 1}.frequency; Sweep_ampl =
data.dev2063.demods.sample{1, 1}.r; Sweep_phase =
data.dev2063.demods.sample{1, 1}.phase*60;

[val, idx] = max(Sweep_ampl);
resonantFreq = Sweep_freq(idx);

ziDAQ('setDouble', '/dev2063/oscs/0/freq', resonantFreq);

ziDAQ('setInt', '/dev2063/demods/1/oscselect', 1); ziDAQ('setDouble',
'/dev2063/oscs/1/freq', FreqAcceleration); ziDAQ('setInt', '/dev2063/demods/0/order', 1);
ziDAQ('setDouble', '/dev2063/demods/0/timeconstant', 0.159154943/LowPassFilter);
ziDAQ('setInt', '/dev2063/demods/1/order', 1);
ziDAQ('setDouble', '/dev2063/demods/1/timeconstant', 0.159154943/LowPassFilter);
ziDAQ('setInt', '/dev2063/demods/0/enable', 1); ziDAQ('setDouble',
'/dev2063/demods/0/rate', SamplingRate); ziDAQ('setInt', '/dev2063/demods/1/enable',
1);
```

```
ziDAQ('setDouble', '/dev2063/demods/1/rate', SamplingRate);

ziDAQ('setDouble', '/dev2063/sigouts/0/amplitudes/0', VdriveResonance); ziDAQ('setDouble',
'/dev2063/sigouts/0/amplitudes/1', VdriveAccel); ziDAQ('setInt', '/dev2063/sigouts/0/enables/1', 1);
ziDAQ('setInt', '/dev2063/sigouts/0/on', 1); [Data] =

getZIPlotterData(SecondsPlotter);



PlotterPhase = Data(:,4); %If error -180
TimePhase = Data(:,1);

OscFreq = interp1(Sweep_phase, Sweep_freq, PlotterPhase);
i=1;
while mean(isnan(OscFreq))>0.2
      OscFreq = interp1(Sweep_phase, Sweep_freq, PlotterPhase-i*180);
      i=i+1;
end

filename = ['OscFreq' num2str(FreqAcceleration) 'Voltage' num2str(VdriveAccel*1000) '. txt'];
fileID = fopen([path filename],'w'); fprintf(fileID,'%d ; %d\n', [TimePhase';
OscFreq']); fclose(fileID);

F = OscFreq;              % Data Channel

X = TimePhase;

dimension = length(OscFreq);

Fs = dimension/X(end); % Sampling frequency
Ts = 1/Fs;             % Sampling period
Fn = Fs/2;             % Nyquist Frequency

F(isnan(F))=[];        % Eliminate 'NaN' Values First

FF = fft(F)/dimension;      % Fourier Series of Data, Freq Vector
Fv = linspace(0,1,fix(dimension/2)+1)*Fn; Iv = 1:length(Fv);
% Index Vector


h = figure();                  % Plot FFT
loglog(Fv, abs(FF(Iv)))
grid
xlabel('Frequency (Hz)')
ylabel('Amplitude')
title("Modulation Frequency of " + num2str(FreqAcceleration) + " Hz" + ' Voltage of ' +
num2str(VdriveAccel*1000))
```

```
xlim([FreqAcceleration-8    FreqAcceleration+8])

filename = ['Freq_' num2str(FreqAcceleration) '_Voltage_' num2str(VdriveAccel*1000) '. fig']; ↙
savefig([path filename]) FFTarray

= abs(FF(Iv));

FFT_peak = max(FFTarray(Fv> FreqAcceleration-0.2 & Fv<FreqAcceleration+0.2)); Noise =

mean(FFTarray(Fv> FreqAcceleration-9 & Fv<FreqAcceleration+10));

fprintf('--Progress %0.0f%%\n', index/length(voltages)* 100);
fprintf('--Frequency: %f\n', FreqAcceleration); fprintf('--Voltage:
%f\n', VdriveAccel); fprintf('--Freq Shift: %f\n', FFT_peak);
fprintf('--Noise: %f\n', Noise);
fprintf('--SNR: %f\n', FFT_peak/Noise);
end
```

B.3 Autocalibration

```
clear all
close all
device_id = 'dev2063';


FreqAcceleration = 160;
%vaccel = linspace(0.1,1, 10);
%vaccel = [0.6, 0.7, 0.8, 0.9, 1];
%vaccel = [0.0250, 0.0500, 0.0750, 0.1000, 0.1250, 0.1500, 0.1750, 0.2000];
%vaccel = [0.05, 0.1, 0.15, 0.2, 0.25, 0.3, 0.35, 0.4, 0.45, 0.5];
vaccel = linspace(0.1,0.8, 8);

rateSamples = 200;
rangeInput = 1.5;

SecondsPlotter = 30;

Voltages = [];

[Data] = getZIPlotterData(2);

index = 0;

for VdriveAccel = vaccel index =

index+1;

ziDAQ('setInt', '/dev2063/demods/1/enable', 0); ziDAQ('setInt',
'/dev2063/sigouts/0/enables/1', 0); ziDAQ('setInt',
'/dev2063/demods/0/enable', 1); ziDAQ('setInt',
'/dev2063/sigouts/0/enables/0', 1);
ziDAQ('setDouble', '/dev2063/sigouts/0/amplitudes/0', VdriveAccel); ziDAQ('setDouble',
'/dev2063/demods/0/rate', rateSamples); ziDAQ('setInt', '/dev2063/demods/0/order', 1);
ziDAQ('setDouble', '/dev2063/demods/0/timeconstant', 1.59154943); ziDAQ('setDouble',
'/dev2063/oscs/0/freq', FreqAcceleration); ziDAQ('setInt', '/dev2063/sigouts/0/on', 1);
%ziDAQ('setDouble', '/dev2063/sigins/0/range', rangeInput);
ziDAQ('setInt', '/dev2063/sigins/0/autorange', 1);

pause(5)

[Data] = getZIPlotterData(SecondsPlotter); PlotterAmplitude

= Data(:,3);

Voltages = [Voltages mean(Data(:,3))];

Accel = Voltages*5e-3*FreqAcceleration*2*pi;

fprintf('Progress %0.0f%%\n', index/length(vaccel)* 100);


end

save Voltages500m.mat Voltages figure()
plot(vaccel, Voltages)
```

B.4 Finding trends

```
clear all
close all
warning off

Accelug=[66.61073109 131.6842915 181.3861446 269.5172658 332.5412652  406.8378499
470.3742395 563.629263];
 Dfr=[0.1289 0.1925   0.241    0.3336   0.6061   0.6798   0.7371   0.7842;
     NaN NaN 0.1278   0.2668   0.1774   0.1535   0.1781   0.2109;
     0.02938 0.07162 0.08828 0.2911   0.4036   0.4818   0.4499   1.034;
     0.1021   0.1666   0.1721   0.1874   0.4136   0.4926   0.7385   0.7529;
     NaN 0.07771 0.1414   0.136    0.2064   0.1875   0.2619 NaN;
0.03774 0.09371 0.08196 0.1553   0.1797   0.2317   0.1564   0.1813;
NaN 0.1246   0.1826   0.1422   0.1653   0.1994   0.216    0.3903;
0.02066 0.02856 0.04044 0.05387 0.02787  0.05441 0.1391   0.1273;
0.04223 NaN 0.09262  0.1353 0.1154    0.2798   0.3506   0.159];

[m,n]=size(Dfr);

for i=linspace(1,m,m)
    D=[Accelug;  Dfr(i,:)];
    D(:,any(isnan(D)))=[];
    f = fit(D(1,:)',D(2,:)','poly1');
    xq = linspace(0,600,500);
    vq = f(xq);
    plot(xq,vq,'-')
    hold on
    title('Interpolation linear')
    xlabel('Acceleration [ug]')
    ylabel('\deltaf_{r} [Hz]')
    legend('1x6','1x9','1x12','3x4','3x8','4x2','4x4','5x1','5x2')
end
```

B.5 Allan deviation

```
function [tau, allandev] = AllanDevLeti2(filename)
data = load(filename);
% data=data1;

time=(data(:,1)-data(1,1));
f=data(:,2);

f0=mean(f); df=f-f0;
Ts=mean(diff(time));
t=[0:Ts:(length(f)-1)*Ts];

H=2*pi*tf([1],[1 0]);
dphi=lsim(H,f,t);

x=dphi/(2*pi*f0);

tau=Ts*[1:floor(length(x)/2)];
sigmay_2=zeros(1,length(tau));

for ii=1:1:length(tau) xtemp=x(1:round(tau(ii)/Ts):length(x));
    ybar=diff(xtemp)/tau(ii);
        for j=1:length(ybar)-1
         sigmay_2(ii)=sigmay_2(ii)+(ybar(j+1)-ybar(j))^2;
    end
    sigmay_2(ii)=1/2*1/(length(ybar)-1)*sigmay_2(ii);
end


allandev=sqrt(sigmay_2);

scrsz = get(0,'ScreenSize');
figure('Position',[scrsz(3)/10 scrsz(4)/10 scrsz(3)/2 scrsz(4)*0.8])
subplot(2,1,1);
plot(t,f*1e-6,'b.');
ylabel('Frequency (MHz)','fontsize',20); xlabel('Time (s)','fontsize',20); title('Raw data','FontSize', 20);
subplot(2,1,2);
loglog(tau,allandev,'b-','LineWidth',2);
ylabel('Allan Deviation','fontsize',20); xlabel('Tau (s)','fontsize',20); title('Allan Deviation','FontSize', 20);
grid(gca,'minor')

filename='Allan_Dev.png';
saveas(gcf,filename);

data2(:,1)=tau;
data2(:,2)=allandev;

DS=dataset(data2);
filename='Allan_Dev.dat';

export(DS,'file',filename,'Delimiter','tab','WriteVarNames',false);

end
```

C Acquired data

C.1 Micro-ship not clamped

			100	200	300	400	500	600	700	800	Acceleration voltages [mV]				
			0,00013	0,000257	0,000354	0,000526	0,000649	0,000794	0,000918	0,0011	cceleration [V]				
			0,000653451	0,001291823	0,001779398	0,002643964	0,00326223	0,003991079	0,004614371	0,005529203	eration [m/s2]				
			66,61073109	131,6842915	181,3861446	269,5172658	332,5412652	406,8378499	470,3742395	563,629263	celeration [ug]				
Rectangle mass 30	1x6	63	0,1289	0,1925	0,241	0,3336	0,6061	0,6798	0,7371	0,7842	Dfr [Hz]	y = 12,84x + 0,0088	12,84	0,203809524	1,999371429
	1x9	28			0,1278	0,2668	0,1774	0,1535	0,1781	0,2109	Dfr [Hz]	y = 6,3848x + 0,1625	6,3848	0,228028571	2,236960286
	1x12	96	0,02938	0,07162	0,08828	0,2911	0,4036	0,4818	0,4499	1,034	Dfr [Hz]	y = 79,49x - 0,177	79,49	0,828020833	8,122884375
Square mass 30	3x4	72	0,1021	0,1666	0,1721	0,1874	0,4136	0,4926	0,7385	0,7529	Dfr [Hz]	y = 60,39x - 0,0626	60,39	0,83875	8,2281375
	3x8	39		0,07771	0,1414	0,136	0,2064	0,1875	0,2619		Dfr [Hz]	y = 46,465x + 0,0323	46,465	1,191410256	11,68773462
Circle mass 30	4x2	45	0,03774	0,09371	0,08196	0,1553	0,1797	0,2317	0,1564	0,1813	Dfr [Hz]	y = 80,694x + 0,0485	80,694	1,7932	17,591292
	4x4	32		0,1246	0,1826	0,1422	0,1653	0,1994	0,216	0,3903	Dfr [Hz]	y = 47,444x + 0,0463	47,444	1,482625	14,54455125
Rectangle mass 25	5x1	78	0,02066	0,02856	0,04044	0,05387	0,02787	0,05441	0,1391	0,1273	Dfr [Hz]	y = 22,719x - 0,006	22,719	0,291269231	2,857351154
	5x2	81	0,04223		0,09262	0,1353	0,1154	0,2798	0,3506	0,1599	Dfr [Hz]	y = 45,659x + 0,0214	45,659	0,563691358	5,529812222
Shape	Emplacement	resonnant frenquency [kHz]										Trendline equation	Slope [Hz/m/s2]	Responsitivity [1/m/s2]	Responsitivity [1/g]

			100	200	300	400	500	600	700	800	Acceleration voltages [mV]				
			1,40E-04	0,000285466	0,000429853	0,000571237	0,000709595	0,000856457	0,001006704	0,001161524	cceleration [V]				
			7,03E-04	0,001434911	0,002160675	0,002871352	0,003566815	0,004305022	0,005060248	0,005838457	eration [m/s2]				
			71,70901396	146,270226	220,2522941	292,6964354	363,589716	438,8401405	515,8254996	595,1536212	celeration [ug]				
Square mass 20	13x1	90		0,07647	0,0545	0,1505	0,133	0,3768	0,2347	0,2872	Dfr [Hz]	y = 59,349x - 0,0264	59,349	0,659433333	6,469041
	13x5	83		0,2253	0,2987	0,3613	0,5345	0,3682	0,4199	0,6031	Dfr [Hz]	y = 37,576x + 0,1579	37,576	0,452722892	4,441211566
Rectangle mass 20	15x2	114			0,09532			0,09245		0,1505	Dfr [Hz]	y = 13,958x + 0,0555	13,958	0,122438596	1,201122632
	15x3	109			0,07208	0,1661	0,04643	0,06931	0,1587	0,1042	Dfr [Hz]	y = 6,4764x + 0,0771	6,4764	0,059416514	0,582876
	15x7	149		0,2323	0,2391	0,3694	0,3075	0,2872	0,1711	0,1914	Dfr [Hz]	y = -17,099x + 0,3185	-17,099	-0,114758389	-1,125779799
	15x9	72	0,1365	0,2204	0,3831	0,4756	0,5373	0,374	0,759	0,8795	Dfr [Hz]	y = 129,96x + 0,0493	129,96	1,805	17,70705
Circle mass 20	11x5	61	0,1388	0,19	0,4602	0,5835	0,6523	1,013	1,339	1,705	Dfr [Hz]	y = 302,11x - 0,2194	302,11	4,952622951	48,58523115
	11x7	42		0,08189	0,1454	0,2074	0,2232	1,017	0,9527	0,5202	Dfr [Hz]	y = 181,54x - 0,2048	181,54	4,322380952	42,40255714
Shape	Emplacement	resonnant frenquency [kHz]										Trendline equation	Slope/ Sensitivity [Hz/g]	Responsitivity [1/m/s2]	Responsitivity [1/g]

			50	100	150	200	250	300	350	400	450	500	Acceleration voltages [mV]				
			7,72E-05	1,46E-04	2,15E-04	2,88E-04	3,63E-04	4,36E-04	5,18E-04	5,77E-04	6,49E-04	7,25E-04	cceleration [V]				
			3,88E-04	7,34E-04	1,08E-03	1,45E-03	1,83E-03	2,19E-03	2,60E-03	2,90E-03	3,26E-03	3,65E-03	celeration [m/s2]				
			39,54040562	74,84915087	110,0929187	147,4495083	186,0523719	223,1876649	265,1804716	295,50813	332,6625932	371,5748449	celeration [ug]				
rectangle mass 30	1x8	74	0,0761		0,2627	0,2003	0,5976	0,6833	0,6953	0,6671	0,5823	0,7678	Dfr [Hz]	= 208,17x + 0,056	208,17	2,813108108	27,59659054
	2x1	87		0,02232	0,04048	0,06925	0,05784	0,0944	0,05257	0,08203	0,1029	0,1151	Dfr [Hz]	= 26,255x + 0,013	26,255	0,301781609	2,960477586
	4x2	53			0,09863	0,147	0,2659	0,1173	0,3093	0,3558			Dfr [Hz]	= 125,82x - 0,03	125,82	2,373962264	23,28856981
Circle mass 30	4x7	64	0,06477	0,05897	0,1906	0,2803	0,4229		0,5818	0,4709	0,4841	0,5812	Dfr [Hz]	= 165,67x + 0,019	165,67	2,58859375	25,39410469
	4x9	48		0,08794	0,1253	0,276	0,3133	0,3102	0,3352	0,6243	0,4328	0,5202	Dfr [Hz]	y = 153,4x + 0,0006	153,4	3,195833333	31,351125
Circle mass 25	9x5	56			0,3184		0,5323	0,3721	0,3486	0,5881	0,5025	1,11	Dfr [Hz]	= 215,01x + 0,001	215,01	3,839464286	37,66514464
Circle mass 20	10x6	61	0,1675	0,2791	0,4434	0,6253	0,5963	0,8203	1,035	1,054	1,251	1,271	Dfr [Hz]	= 354,46x + 0,042	354,46	5,810819672	57,00414098
	10x10	104	0,09867	0,189	0,3477	0,4751	0,54235	0,6886	0,8131	0,6607	0,6806	0,9943	Dfr [Hz]	y = 238,1x + 0,0711	238,1	2,289423077	22,45924038
Shape	Emplacement	resonnant frenquency [kHz]											Trendline equation	Slope/ Sensitivity [Hz/m/s2]	Responsitivity [1/m/s2]	Responsitivity [1/g]	

C.2 Micro-ship clamped

			100	200	300	400	500	600	700	800	Acceleration voltages [mV]				
			0,000139	0,00028	0,000417	0,000563	0,000708	0,000847	0,000991	0,001137	Acceleration [V]				
			0,000696	0,001408	0,002095	0,002828	0,003558	0,004258	0,00498	0,005714	Acceleration [m/s2]				
			70,96721	143,5503	213,589	288,3227	362,6538	434,0571	507,6553	582,4461	Acceleration [ug]				
Square mass 30	3x4	75	0,05699	0,1306	0,3427	0,2796	0,3825	0,4059	0,8599	0,4005	Dfr [Hz]	y = 105,08x + 0,0219	105,08	1,401066667	13,744464
Circle mass 30	4x2	47	0,04338	0,05539	0,0822	0,1732	0,2376	0,1488	0,1964	0,2145	Dfr [Hz]	y = 43,121x + 0,028	43,121	0,917468085	9,000361915
	4x5	69	0,1019	0,1929	0,3113	0,2386	0,4239	0,5908	0,633	0,7337	Dfr [Hz]	y = 152,32x - 0,0061	152,32	2,207536232	21,65593043
Circle mass 20	11x5	63		0,03879	0,04666	0,09989	0,1729	0,1136	0,1612	0,1881	Dfr [Hz]	y = 34,406x - 0,0048	34,406	0,546126984	5,357505714
	11x7	76		0,06373	0,1048	0,1102	0,1689	0,2194	0,2377	0,2201	Dfr [Hz]	y = 41,911x + 0,012	41,911	0,551460526	5,409827763
Square mass 20	13x1	90	0,03909	0,07795	0,2809	0,226	0,1577	0,4717	0,1462	0,2733	Dfr [Hz]	y = 40,976x + 0,0783	40,976	0,455288889	4,466384
	13x5	68		0,08906	0,1108	0,03364	0,1449	0,2097	0,212	0,1377	Dfr [Hz]	y = 25,992x + 0,0417	25,992	0,382235294	3,749728235
Shape	Emplacement	resonnant frenquency [kHz]										Trendline equation	Slope/ Sensitivity [Hz/m/s2]	Responsitivit y [1/m/s2]	Responsitivity [1/g]

C.3 Micro-ship clamped: Circle devices

						100	200	300	400	500	600	700	800	Acceleration voltages [mV]				
						0,000153	0,000309	0,000463	0,000614	0,000778	0,00093	0,001084	0,00125	Acceleration [V]				
						0,000771	0,001553	0,002329	0,003085	0,003913	0,004672	0,005451	0,006284	Acceleration [m/s2]				
						78,54431	158,3175	237,4092	314,5014	398,8646	476,295	555,6214	640,5952	Acceleration [ug]				
Circle mass 30	4x2	1,02E+08	2,23E+07	47	22	0,04338	0,05539	0,0822	0,1732	0,2376	0,1488	0,1964	0,2145		y = 36,025x + 0,0289	43,121	0,917468085	9,000361915
	4x5	2,19E+08	1,94E+08	69	65	0,1019	0,1929	0,3113	0,2386	0,4239	0,5908	0,633	0,7337		y = 127x - 0,0021	152,32	2,207536232	21,65593043
	4x7	1,39E+08	1,24E+08	55	52	0,1048	0,1573	0,2691	0,3897	0,4395	0,5834	0,6575	1,008		y = 183,42x - 0,0751	183,42	3,371272727	33,07218545
	4x12	1,83E+08	1,39E+08	63	55		0,113	0,1235	0,1514	0,3268	0,1772	0,3235	0,5734		y = 103,12x - 0,0697	103,12	1,636825397	16,05725714
	4x14	2,73E+08	1,88E+08	77	64	0,05472	0,1215	0,3191	0,3366	0,4234	0,2506	0,7662	1,085		y = 195,36x - 0,1348	195,36	2,537142857	24,88937143
	4x10	5,96E+07	2,23E+07	36	22			0,01581	0,006945	0,02382	0,01325		0,0348		y = 5,1863x - 0,0021	5,1863	0,144063889	1,41326675
Circle mass 25	8x3	7,29E+07	7,63E+07	44	45	0,0432	0,05529	0,06617	0,07518	0,11	0,05723	0,07852	0,2608		y = 25,194x + 0,0049	25,194	0,572590909	5,617116818
	8x4	2,66E+08	2,35E+08	84	79	0,1388	0,157	0,5633	0,472	0,3672	0,5161	0,6605	0,9369		y = 119,22x + 0,0583	119,22	1,419285714	13,92319286
	8x5	1,18E+08	1,02E+08	56	52	0,1241	0,2188	0,4022	0,4123	0,5653	0,6662	0,9749	1,786		y = 248,97x - 0,2295	248,97	4,445892857	43,61420893
	8x7	7,97E+07	3,39E+07	46	30	0,0901	0,08909	0,1692	0,2178	0,2349	0,2331	0,4081	0,4948		y = 70,39x - 0,0047	70,39	1,530217391	15,01143261
	9x15	1,59E+08	1,40E+08	65	61		0,05816	0,04399		0,08568	0,03772	0,08944			y = 6,0117x + 0,0415	6,0117	0,092487692	0,907304262
	9x14	1,79E+08	1,54E+08	69	64	0,09547	0,2196	0,2701	0,3891	0,5599	0,9068	0,3313	0,1978	Dfr [Hz]	y = 50,375x + 0,1946	50,375	0,730072464	7,16201087
	9x13	3,86E+07	4,10E+07	32	33				0,07212		0,05172		0,2257		y = 48,164x - 0,1089	48,164	1,505125	14,76527625
	9x7	8,32E+07	7,63E+07	47	45	0,08054	0,2037	0,1378	0,286	0,5378	0,6754	0,6005	0,5368		y = 106,67x + 0,0082	106,67	2,269574468	22,26452553
Circle mass 20	10x2	8,24E+07	7,34E+07	53	50	0,07705	0,2388	0,4321	0,2166	0,6268	0,43	0,8463	1,493		y = 203,51x - 0,1687	203,51	3,839811321	37,66854906
	10x3	1,65E+08	1,65E+08	75	75				0,1017	0,1412	0,116	0,3687	0,252		y = 66,033x - 0,1132	66,033	0,88044	8,6371164
	10x5	1,13E+08	1,13E+08	62	62	0,1694	0,3403	0,4334	0,4315	0,171	0,6329	1,756	1,843		y = 290,36x - 0,2962	290,36	4,683225806	45,94244516
	10x6	1,32E+08	7,93E+07	67	52		0,3514	0,3291	0,2557	0,3818	0,5725	0,6632	0,9461		y = 126,25x + 0,0078	126,25	1,884328358	18,48526119
	10x7	1,24E+08	1,02E+08	65	59		0,1508	0,2756	0,2335	0,3755	0,4461	0,5393	0,7866		y = 120,57x - 0,069	120,57	1,854923077	18,13679538
	10x11	1,24E+08	1,16E+08	65	63	0,08466	0,1484	0,1675	0,167	0,4112	0,2308	0,2443	0,5213		y = 60,598x + 0,0344	60,598	0,932276923	9,145636615
	11x5	1,16E+08	9,53E+07	63	57		0,08345	0,193	0,1095	0,3703	0,3365	0,5044	0,4459		y = 88,039x - 0,0513	88,039	1,397444444	13,70893
	11x5	1,16E+08	9,53E+07	63	57		0,03879	0,04666	0,09989	0,1729	0,1136	0,1612	0,1881		y = 34,406x - 0,0048	34,406	0,546126984	5,357505714
	11x7	1,69E+08	1,24E+08	76	65		0,06373	0,1048	0,1102	0,1689	0,2194	0,2377	0,2201		y = 41,911x + 0,012	41,911	0,551460526	5,409827763
Shape	Emplacement	Membrane stress [Pa]	Membrane stress after annealing [Pa]	resonnant frenquency [kHz]	resonnant frenquency after annealing [kHz]										Trendline equation	Slope/ Sensitivity [Hz/m/s2]	Responsitivity [1/m/s2]	Responsitivity [1/g]

C.4 Micro-ship annealed: Circle devices

					100	200	300	400	500	600	700	800	Acceleration voltages [mV]				
					0,00017976	0,00034572	0,00053078	0,00070518	0,00089424	0,00106813	0,00125194	0,00144617	Acceleration [V]				
					0,00090357	0,00173776	0,00266799	0,00354463	0,00449493	0,00536901	0,00629293	0,00726926	Acceleration [m/s2]				
					92,1072587	177,141697	271,965856	361,328132	458,198954	547,299625	641,480703	741,004753	Acceleration [ug]				
Circle mass 30	4x5	2,19E+08	1,94E+08	71		0,07497	0,07703	0,1675	0,2414	0,5562	0,2705	0,1398		y = 32.304x + 0.0478	32,304	0,45498592	4,463411831
	4x7	1,39E+08	1,24E+08	54		0,09993	0,2244	0,5246	0,6178	0,4891	0,4627	0,7459		y = 80.816x + 0.0258	80,816	1,49659259	14,68157333
	4x14	2,73E+08	1,88E+08	77	0,194	0,4078	0,7247	0,5842	1,372	1,142	0,5806	0,5948		y = 64.053x + 0.3961	64,053	0,83185714	8,160518571
Circle mass 25	8x3	7,29E+07	7,63E+07	49	0,07018	0,1373	0,3782	0,4894	0,3078	0,317	0,6882	0,3544		y = 56.772x + 0.1137	56,772	1,15861224	11,36598612
	8x5	1,18E+08	1,02E+08	55	0,1413	0,1692	0,3843	0,4066	0,4776	0,8484	0,5085	0,8402		y = 105.38x + 0.0468	105,38	1,916	18,79596
	9x15	1,59E+08	1,40E+08	64			0,05964		0,1148	0,1098	0,1774	0,08736	Dfr [Hz]	y = 12.161x + 0.0463	12,161	0,19001563	1,864053281
	9x14	1,79E+08	1,54E+08	68			0,1653	0,2008	0,2208	0,2631	0,3789	0,2608		y = 32.498x + 0.0877	32,498	0,47791176	4,688314412
	9x7	8,32E+07	7,63E+07	47		0,1503	0,2034	0,4318	0,5694	0,6419	1,543	1,682		y = 253.08x - 0.589	253,08	5,38468085	52,82371915
Circle mass 20	10x2	8,24E+07	7,34E+07	53	0,1074	0,2714	0,219	0,388	0,327	0,9885	0,1593	0,4935		y = 56.859x + 0.1398	56,859	1,07281132	10,52427906
	10x5	1,13E+08	1,13E+08	62		0,1579	0,1996	0,7443	0,5728	0,3281	0,6091	0,7702		y = 87.27x + 0.092	87,27	1,40758065	13,80836613
	11x5	1,16E+08	9,53E+07	61		0,143	0,1332	0,2852	0,3553	0,3358	0,2926	0,1734		y = 17.575x + 0.1667	17,575	0,28811475	2,826405738
	11x7	1,69E+08	1,24E+08	76	0,1081	0,2088	0,2594	0,2784	0,5089	0,793	0,6609	2,048		y = 233.11x - 0.3324	233,11	3,06723684	30,08959342
Shape	Emplacement	Membrane stress [Pa]	Membrane stress after annealing [Pa]	resonnant frenquency [kHz]										Trendline equation	Slope/ Sensitivity [Hz/m/s2]	Responsitivity [1/m/s2]	Responsitivity [1/g]